Author(s): Kiejna, A. & Nieminen, Risto M.

Title: Energetics of Sr adatom interactions on the Mo(112) surface

Year: 2004

Version: Final published version

Energetics of Sr adatom interactions on the Mo(112) surface

A. Kiejna[1,2] and R. M. Nieminen[2]
[1]*Institute of Experimental Physics, University of Wrocław, Plac M. Borna 9, PL-50-204 Wrocław, Poland*
[2]*Laboratory of Physics, Helsinki University of Technology, P.O. Box 1100, FIN-02015 HUT, Finland*
(Received 25 January 2004; revised manuscript received 2 April 2004; published 30 June 2004)

First-principles methods are used to investigate the formation and structure of the ordered phases of Sr atoms adsorbed on the furrowed Mo(112) surface. The energetics of various commensurate and incommensurate adatom structures providing information on lateral interactions between adatoms is determined for coverages $0.11 \leqslant \Theta \leqslant 1$ monolayer. It is found that the binding energy of Sr atoms decreases with increasing coverage. The experimentally observed $p(8\times1)$ and $p(5\times1)$ adatom chains are found to belong to the most favored structures for $\Theta < 0.5$. The energetic difference between these two structures amounts to 20 meV. The experimental work function variation with Sr adatom coverage is very well reproduced. The energy barriers for Sr diffusion along the atomic troughs are calculated and discussed.

DOI: 10.1103/PhysRevB.69.235424 PACS number(s): 68.43.Bc, 68.35.Bs, 68.43.Fg, 73.30.+y

I. INTRODUCTION

The presence of surface atomic steps and terraces may drive the growth of specific adatom structures. Adatoms usually gather in linear chains decorating the steps. The bcc (112) surface has a furrowed structure in which atoms can adsorb along close-packed $[11\bar{1}]$ directions. Extensive experimental studies of submonolayer adsorption of metallic atoms on the (112) surface of tungsten and molybdenum discovered a diversity of ordered adatom structures that provide evidence for a strong anisotropy of lateral interactions. For example, Au and Pd atoms form long atomic chains following the furrows.[1,2] The occupied troughs are separated by three or two unoccupied ones, for Au and Pd, respectively, while the Pt-atom chains are distributed at random. Some other metals, for example Ag and Ni, do not form chains. The self-assembly of atomic chains (nanowires) is a manifestation of the attractive interaction between atoms in the same furrow. On the other hand, the presence of unoccupied troughs suggests a repulsive interaction between atomic chains across the furrows.

Although the structure of atomic chains to a large extent is dictated by that of the underlying surface, they do not necessarily follow the direction of the troughs. Alkali and alkaline-earth metal atoms adsorbed in the furrows of Mo(112)) and W(112) form quasi-one-dimensional commensurate chain structures of the $p(n\times1)$ type, aligned normal to the furrows.[3] The structures are observed for coverages smaller than 0.5 monolayer (ML) and their periodicity n along the substrate rows can vary from 2 to 4 for Li/Mo(112) and up to 9 for a Sr/Mo(112),[4–9] where the chains can be separated by as much as 25 Å. Thus, for low coverages of alkali-metal adsorbates, the repulsive adatom-adatom interaction prevails[10] at short distances along the furrows, with possible attractive minima at larger distances of n surface lattice constants. In the direction perpendicular to the furrows this repulsive interaction is to a large extent screened by the substrate atoms, and the attractive and repulsive components can be balanced leading to formation of commensurate structures. For coverages exceeding 0.5 ML, incommensurate structures were reported although long-range order of these structures is still possible.

The coupling mechanism between alkali-atom chains on the W and Mo(112) surface is often explained by a hybrid model of the dipole-dipole repulsive interactions mediated by the local distortion in the substrate electron distribution induced by the adsorbed atoms.[8] This distortion is screened by adsorbate induced Friedel oscillations of the electron distribution and leads to an indirect interaction potential of a long-range oscillatory character. The minima in the adatoms interaction potential have a periodicity of twice the Fermi wave number and thus their positions depend on the substrate band structure. Lattice-gas model simulations [11,12] have shown the applicability of such a potential to describe the stable phases. Understanding of the subtle mechanism of the coupling leading to the formation of atomic chains requires, however, a more quantitative analysis of their energetics based on accurate *ab initio* calculations.

The long periodicity of chain structures makes them difficult to treat by first-principles methods. Such calculations performed by present authors[13] for the Li/Mo(112) system have demonstrated a predominance of the Li-Mo adsorbate-substrate chemisorption interactions over the weak lateral Li-Li interactions. The results of these extensive calculations of binding energies of a variety of configurations have shown that chain structures are the most favored ones. Based on our *ab initio* results, Drautz *et al.*[14] examined 10^8 different adatom configurations using cluster expansion techniques and found that the lowest energy structures coincided with ours. To disentangle the mechanism behind the formation of different adsorbate phases first-principles calculations are necessary.

In this work, we report on results of extensive first-principles calculations for various configurations and coverages for the Sr/Mo(112) system. Our focus is on the ordered structures of the Sr adlayers corresponding to coverages of up to 1 ML. Section II outlines the methodology of calculations. In Sec. III we discuss our results, and Sec. IV provides a brief summary.

II. DETAILS OF CALCULATION

The calculations employ density-functional theory (DFT)[15,16] in the generalized gradient approximation for the exchange-correlation energy functional,[17] a plane wave basis set and the projector augmented-wave (PAW) potentials[18] as implemented in the Vienna *Ab initio* Simulation Package (VASP),[19] which allow an accurate treatment of the considered system. A plane wave basis energy cutoff of 250 eV is applied. The Mo(112) substrate is modeled by periodic slabs consisting of seven molybdenum layers (≈9 Å thick) separated by eight equivalent layers of vacuum. The Sr atoms are adsorbed on one side of the slab and an artificial electric field arising due to the asymmetry of the system is compensated by a dipole correction.[10] The coordinates of atoms in the four topmost molybdenum layers, and of all the adsorbed atoms, are optimized until the forces on unconstrained atoms converge to less than 0.025 eV/Å. The equivalent mesh $20\times12\times1$ of 60 Monkhorst-Pack[20] special **k**-points is used to sample an irreducible wedge of the Brillouin zone of the $1\times1\times(7+8)$ orthorhombic unit cell (and proportionally reduced depending on the size of supercell). To improve the convergence, for the fractional occupancies a Methfessel-Paxton method[21] with a broadening of 0.2 eV is applied.

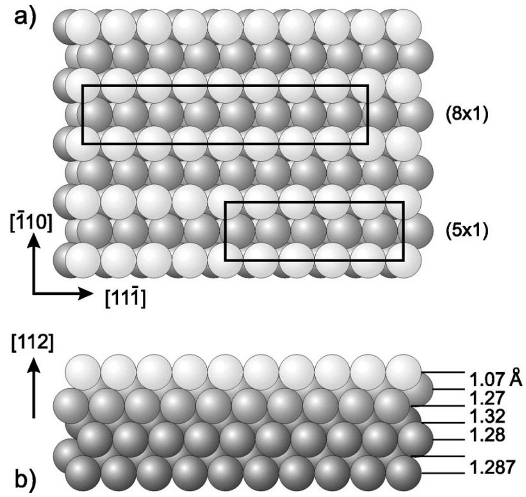

FIG. 1. (a) Top view of the Mo(112) surface showing the directions of the atomic furrows and two surface unit cells applied in the calculations. (b) Side view of the seven Mo layer slab. The numbers to the right show the calculated interplanar separations (in Å) of the topmost layers. The bottom number is for the bulk interplanar spacing.

III. RESULTS AND DISCUSSION

A. Clean Mo(112) surface

The bulk and bare metal-surface structural parameters were determined by us previously,[13] but in order to check the difference, which might result from the replacement of ultrasoft pseudopotentials by the PAW potentials, they were recalculated here. The calculated lattice parameter of bcc Mo is 3.152 Å; i.e., it is the same as determined by us previously,[13] in perfect agreement with the experimental value 3.15 Å,[22] and local density approximation (LDA) calculations (3.16 Å),[23] while the bulk modulus (260 Mbar) is 3% higher compared to the pseudopotential calculation.[13]

Figure 1 displays the atomic arrangements of the (112) surface slab of a bcc crystal. The results reported here for a 1×1 surface unit cell of the vicinal Mo(112) agree well with our earlier results.[13] A furrowed (112) surface shows, in accordance with the predictions of a simple electrostatic model,[24,25] a 17% contraction of the interplanar distance for the topmost atomic plane, in very good agreement with our previous work (−17.7%),[13] other recent first-principles calculations,[23] and experimental values.[26] Vertical relaxation of deeper layers is relatively small and amounts to −0.93% (−1.2%), 3.0% (2.9%), and −0.31% (−0.36%) for the second, third, and fourth interlayer spacing, respectively, and are very similar to those determined by us in Ref. 13, which are quoted in parentheses. Denoting by minus and plus signs contraction and expansion, respectively, the multilayer relaxation pattern as a function of increasing depth from the surface can be written[13] in the form $--+-$, which disagrees with a $-+-+$ sequence determined by another DFT LDA calculation[23] and experiment.[26] This discrepancy, which concerns deeper Mo layers, may arise partially from the different exchange-correlation functionals applied and has a negligible effect on the adsorption process. Lateral shifts of the surface layers as a whole are small and are not altered compared to our previous work.

The calculated surface energy amounts to 2.38 eV/atom and is slightly smaller than the value reported[23] for the LDA. The work function for the relaxed surface calculated for various supercells is equal to 4.11−4.12 eV. This is ∼3% smaller than that determined by us previously, and 5% less than the experimental work function (4.36 eV) measured by photoemission.[27]

B. Surface structures of Sr/Mo(112)

In this subsection, we discuss the changes in the surface structure and the electronic properties of the clean Mo(112), induced by Sr atoms of coverages $1/9\leqslant\Theta\leqslant1$. Coverage Θ is defined as the ratio of the number of adatoms to the number of substrate atoms in a surface unit cell. Based on our previous calculations and on experiment,[5] from the outset we limit the number of possible atomic configurations, and assume that the most favored adsorption sites for Sr atoms are the positions that would be occupied by atoms of an additional substrate layer; i.e., the bulk (volume) sites. However, for some of the considered Sr coverages/structures, the second or third adatom was initially located in a bridge or hollow site. In most cases they are unstable, and the atoms shifted towards volume positions.

To account for the long-range character of lateral interactions that lead to the formation of the low-coverage structures of the $p(n\times1)$ type, with $n\leqslant9$, large surface unit cells have to be applied (cf. Figs. 1 and 2). Table I presents the binding energies E_b with respect to the energy of a free Sr atom, calculated for different coverages and a variety of surface unit cells considered. Note that the binding energy, which is calculated from the total energy difference of the

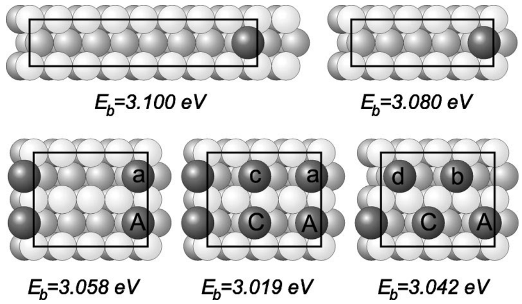

FIG. 2. Geometry of a single Sr adatom on the Mo(112) surface in the 8×1 and 5×1 unit cells (upper row), and two and four Sr adatoms in the 4×2 cell. Atoms are adsorbed at the bulk sites in atomic furrows. Adatoms belonging to the same furrow are denoted either by upper or lower case letters. The labeling corresponds to that adopted in Table I. The binding energy of the Sr adatom corresponding to a given configuration is printed below.

systems with and without adsorbate, is defined here as positive.[13] Similarly as for the Li/Mo(112) system, for low coverages the chainlike structures are favored. The strongest binding is found for the atoms in a $p(9\times1)$ chain. This pattern was discarded by recent measurements[7] in favor of the $p(8\times1)$ structure, which, according to the present calculations, is slightly less stable. For a higher coverage ($\Theta=0.5$) a more homogeneous distribution of Sr atoms, such as the $c(2\times2)$ structures (ACbd pattern in Fig. 2) becomes favored over linear chains. The energetic differences usually amount to several tens of meV. Thus, they are two orders of magnitude smaller than the Sr-Mo-substrate chemisorptive binding. For the most strongly bound atom in the (9×1) structure, and the most weakly bound atoms in the 4×2 unit cell, this difference is ~250 meV. Sr atoms bind more strongly to the Mo substrate than Li atoms do. For small coverages [$p(8\times1)$ structures], the difference in the binding amounts to 220 meV and for higher coverages drops to 160 meV.

The binding energies calculated for the same coverage of Sr atoms in unit cells of different sizes and for different number of **k**-points allow to estimate the error bars. The values of E_b for a single Sr atom in the 4×1 and two evenly spaced Sr atoms in 8×1 cell differ by about 6 meV (Table I). Similarly, for the (4×1) structure of 2 Sr atoms in the 8×1 and 4×2 cells (AE and Aa structures with $2\times12\times1$ and $5\times6\times1$ **k**-point meshes, respectively), one obtains binding energies that agree to within 6 meV. Thus, the accuracy in the determination of the relative energies in different unit cells amounts to about ±5 meV.

Calculations of the binding energy of two Sr atoms performed for the fixed coverage $\Theta=1/4$ but in two different surface unit cells [8×1, and 4×2 (Fig. 2)], clearly show (Table I) that for this coverage, the formation of the $p(4\times1)$ chain structures across the rows is favored over clustering along the rows and over the zigzag and rectangular-centered structures. We conclude that, similar to the Li/Mo(112) system,[13] the bonding of Sr adatoms and the stability of their structures enhances with aligning adatoms normal to the furrows.

The geometries of some stable structures for coverages 1/8, 1/5, and 1/4 ML are presented in Fig. 2. For a higher coverage ($\Theta=1/2$ ML), the Sr atoms do not form $p(2\times1)$ chains (ACac), but instead form a $c(2\times2)$ configuration (ACbd). These results and the more extended data of Table II show that the energetic difference between the chain structures, which can be considered as a measure of amplitude of the lateral Sr-Sr interactions on Mo(112), is below 100 meV. Note that this is approximately tripled compared to the Li-Li adatom interactions.[13] In case of Li adatoms, whose size is similar to Mo atoms, the repulsive interaction across the furrows is screened by the substrate and the formation of $p(2\times1)$ chains is possible. The larger Sr atoms protrude above the top Mo rows and the screening is much less effective. Consequently, to balance the repulsive interactions along and across the furrows a $c(2\times2)$ structure of hexagonal symmetry (Fig. 2) is formed.

For the most favored linear-chain structures, a decrease in the binding energy with increasing coverage is clearly seen (Table II). While for $\Theta\leqslant1/2$ the changes in the binding energy do not exceed 0.1 eV, they grow rapidly for $\Theta\geqslant3/5$ and amount to 1.6 eV for a full monolayer coverage.

TABLE I. Binding energies of Sr atoms on Mo(112) for different coverages and sizes of surface unit cells applied in the calculations. The position of a single Sr atom in a volume site is denoted by A, and the subsequent volume sites by B, C, D, etc. The corresponding sites in a neighboring furrow are labeled by lower case letters, respectively. The binding energies of same Sr structures and coverages calculated in different unit cells are printed in bold face.

Coverage (ML)	Surface cell	Sr atom positions	E_b(eV)
1/9	9×1	A	3.117
1/8	8×1	A	3.100
	4×2	A	2.957
1/6	6×1	A	3.083
1/5	5×1	A	3.080
1/4	4×1	A	**3.058**
	8×1	AE	**3.052**
	8×1	AB	3.022
	8×1	AC	3.054
	8×1	AD	3.047
	4×2	AC	2.867
	4×2	Ac	2.895
	4×2	Ab	3.013
	4×2	AB	2.867
	4×2	Aa	**3.058**
	4×2	Ad	3.013
1/3	6×1	AD	3.025
1/2	4×1	AC	**3.019**
	6×1	ACE	**3.016**
	8×1	ACEG	**3.013**
	4×2	ACac	**3.019**
	4×2	ACbd	3.042
3/5	5×1	ACE	2.997
3/4	4×1	ABC	2.744
1	4×1	ABCD	1.485

TABLE II. Binding energies of Sr atomic chains adsorbed on Mo(112) for different coverages and surface unit cells. $d_{\mathrm{Sr},1}$ and $d_{\mathrm{Sr},2}$ denote the average distance of a Sr adatom to the topmost and second Mo layer, respectively. ΔE_b is the difference in binding energies E_b per Sr adatom with respect to the binding for the coverage $\Theta = 1/9$ ML.

Coverage (ML)	Surface cell	Adatom distance $d_{\mathrm{Sr},1}$(Å)	$d_{\mathrm{Sr},2}$(Å)	E_b (eV)	ΔE_b (eV)
1/9	9×1	2.15	3.23	3.117	0.000
1/8	8×1	2.14	3.22	3.100	−0.017
1/6	6×1	2.14	3.22	3.083	−0.034
1/5	5×1	2.13	3.21	3.080	−0.037
1/4	4×1	2.14	3.22	3.058	−0.059
1/3	6×1	2.13	3.21	3.025	−0.092
1/2	4×1	2.14	3.23	3.019	−0.098
3/5	5×1	2.17	3.26	2.997	−0.120
3/4	4×1	2.18	3.27	2.744	−0.373
1	4×1	2.06	3.16	1.485	−1.632

A magnitude of this variation for $\Theta < 3/5$ is enhanced compared to the Li/Mo(112) adsorption and suggests a stronger interaction of the Sr atoms with the Mo substrate. The decrease in the binding energy with coverage is in general accompanied by a small decrease in the vertical distance of the Sr adatom to the underlying Mo plane. The changes are not regular, however. Interestingly, a dramatic change in the binding energy which occurs for $\Theta = 1$ (E_b is halved compared to the $\Theta \leqslant 3/4$ ML case), is only weakly reflected in a change of the vertical Sr-Mo-layer distance, which is reduced by 0.06 and 0.08 Å (to second and first layer, respectively). This reduction of the vertical bond length of Sr adatoms in the fivefold coordinated volume positions is similar to that reported by us for Li/Mo(112) system,[13] and differs from the trend observed for alkali-atom adsorption on simple metal surfaces.[28]

The Sr atoms, similar to Li atoms, have a stabilizing effect on the Mo(112) surface. It is manifested in a diminished contraction of the average interlayer distance between the topmost Mo layers with increasing Sr coverage (Table III), from −17% for a clean Mo(112), down to −14.4% for $\Theta = 1$. Interestingly, the relaxations of the deeper Mo layers,

TABLE III. Change in the average geometry of the four uppermost layers of Sr/Mo(112) system. Δd_{ij} are the vertical relaxations of interlayer distance (in % of the bulk interlayer spacing).

Coverage	Cell	Δd_{12}	Δd_{23}	Δd_{34}	Δd_{45}
0	1×1	−17.0	−0.93	3.0	−0.31
1/9	9×1	−16.7	−0.22	2.5	−0.42
1/8	8×1	−16.6	−0.33	2.4	−0.43
1/5	5×1	−16.4	0.30	2.0	−0.42
1/4	4×1	−16.0	0.61	1.9	−0.54
1/2	4×1	−15.5	2.3	0.55	−0.41
1	4×1	−14.4	5.1	−1.7	−0.02

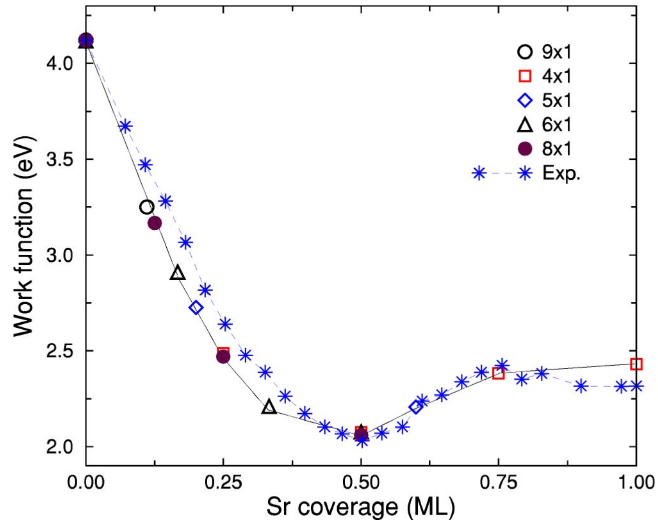

FIG. 3. (Color online) Calculated work function changes for the Sr/Mo(112) adsorption compared with the measured data (asterisks) of Ref. 5 For each coverage only the work function values of the most stable chain structures (calculated in different surface unit cells of $n \times 1$ type) are plotted.

although smaller in magnitude, vary more radically, changing even their sign. This results in a reordering of the $--+-$ relaxation pattern for a clean surface into a $-+-\pm$ sequence for 1 ML of Sr atoms. The vertical shifts of the atoms of the particular Mo layers relative to the center-of-mass position are small and do not exceed 0.04 Å.

The work function variation due to Sr adsorption in the most stable structures (Table I) for a given coverage is displayed in Fig. 3 and compared with experiment. Both dependencies are calibrated by setting the experimental work function for the clean Mo(112) equal to the calculated value (4.11 eV). The calculated data follow a smooth curve which shows a variation typical of alkali metal adsorption[29] as explained by the classical Langmuir-Gurney picture.[28] Both the overall shape and the position of a minimum in the experimental $\Delta\Phi(\Theta)$ curve at $\Theta = 0.5$ ML, as well as the magnitude of the work function lowering of about 2 eV, for $0 \leqslant \Theta \leqslant 0.5$ are very well reproduced.[5] The magnitude of the initial dipole moment, which can be measured by the slope of the curve for $\Theta \leqslant 0.25$, is approximately doubled compared to the Li/Mo(112) system.[13] The maximum work function lowering is 70% larger for Sr/Mo(112) adsorption. It agrees with a common view that the larger the atomic radius of the adsorbate the further away from the surface is the ionized atom and the larger is the induced dipole moment. This geometrical effect is additionally enhanced by a larger electron transfer from Sr to Mo than that from Li to Mo. In addition, the value of work function for 1 ML coverage (2.43 eV), that corresponds to metalization of the adlayer, agrees well with the experimental work function for polycrystalline Sr.[29]

It is worth noting that at 1 ML coverage, the calculated binding energy (Table II) is smaller than the heat of formation of Sr crystal (1.72 eV).[22] This supports the view that under usual experimental conditions the second layer starts to form before the monolayer coverage is reached. Therefore, the experimental data in Fig. 3 do not correspond to the calculated geometry, although they still agree quite well. It means that work function is rather insensitive to the long-range order in adsorbate layer.

C. Low-coverage Sr structures

The results of (Table I) show that for $\Theta < 0.5$ the commensurate chains formed of Sr adatoms are favored. This agrees with experimental observations[6] which predict stable (8×1) and (5×1) Sr structures in this range of coverages. The former structure is also suggested by our calculation but is characterized by a slightly smaller binding than the $p(9\times1)$ one. The Sr-(9×1) structure, which is 17 meV more stable than the $p(8\times1)$, was also reported in an earlier experimental study,[9] but is not confirmed by a more recent one.[7] On the other hand, the $p(8\times1)$ is only commensurate at temperatures below 125 K and grows as islands. The average size of the islands at their first appearance at $\Theta = 0.07$ is around 24 Å, which corresponds to multiplicity $n=9$ of surface lattice constants $a_{11\bar{1}}$ (Ref. 6). Thus, the discrepancy between theory and experiment may result from the fact that calculations are performed for a globally homogeneous coverage, whereas experiment deals with more local coverages.

According to experiment,[6] already at coverages $\Theta \approx 0.25$, the $p(5\times1)$ structures are replaced by islands with $c(2\times2)$ structure which, eventually, form a stable single phase at $\Theta \approx 0.5$. It seems that this finds support in our results. As it is seen from Table I, the $c(2\times2)$, or ACbd structure in nomenclature of Table I, and some other structures for $\Theta = 0.25$ are characterized by similar binding energies.

Interestingly, although the energy differences between particular structures for the Sr/Mo(112) system are, in general, distinctly larger than for the Li/Mo(112),[13] the two stable but different configurations that are observed in each of the systems [i.e., Sr-(8×1) and (5×1), and Li-(4×1) and (2×1)], differ by the same amount of energy ($\approx$20 meV).

In order to analyze the stability of different linear structures, it is interesting to plot the binding energy differences vs coverage for lower coverages (Fig. 4). The plotted changes in the binding energy with the increasing coverage corresponding to structures (chains) of smaller periodicity, show an interesting phase stability diagram in the form of "devil's staircase" in which commensurate phases are separated by incommensurate phases.[30] As is seen, for coverages $0.17 \leqslant \Theta \leqslant 0.5$, one can distinguish two regions of stable chains which differ by $\approx$5 meV in the binding energy (i.e., the differences are within the limits of accuracy of our calculations). Among the two Sr structures, namely, the $p(6\times1)$ and $p(5\times1)$, experiment suggests that the latter is stable. Our results indicate that formation of this structure is, probably, preceded by an equally favored $p(6\times1)$ phase, which may coexist with $p(5\times1)$ in some regions of the surface. According to our diagram, another region of stable chain-phases should appear for $1/3 \leqslant \Theta \leqslant 1/2$. An inspection of Table I shows that the Sr-$p(2\times1)$ is by $\sim$20 meV less favored than the $c(2\times2)$ one. In addition the $p(3\times1)$ structure is not observed experimentally. However, experiment shows that both the $p(2\times1)$ and $p(3\times1)$ can be stabilized when small amounts of oxygen (of surface concentration $\sim$12%) is present at the surface. The same applies to the $p(9\times1)$ chains. Thus, it seems that our phase stability diagram (Fig. 4) predicts the regions of coverages for which stable commensurate structures of Sr adsorbate should appear.

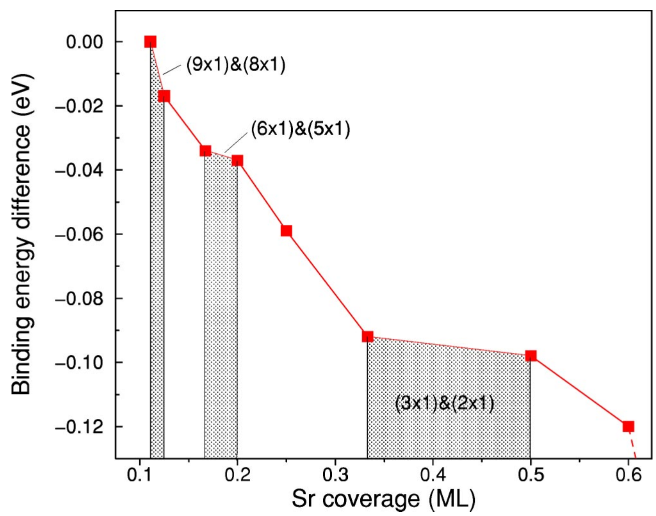

FIG. 4. Binding energy differences (compare Table II) vs coverage, showing the surface phase diagram of stable (gray) and unstable chain structures for low Sr coverages.

Finally, let us note that the stability of one or the other phase should always be considered with respect to the possibility of mixing. This means that phases such as (3×1) and (6×1) are unstable towards mixing into coexistence of $c(2\times2)$ and (5×1), and (5×1) and (8×1) phases, respectively. As is seen from Fig. 4, and also observed in experiment,[31] the average binding energy for the coexisting phases is higher than for the pure phases.

As already mentioned, the Sr atoms bind about 0.2 eV stronger to Mo than Li atoms. This seems not to have much effect on the Sr-Mo bond length, which is increased compared to the Li-Mo bond by the amount equal to the difference ($\simeq$0.6 Å) in metallic radii of Sr and Li (Fig. 5). For the Sr-(5×1) system, the binding of Sr to the Mo atom of the second Mo layer agrees with experiment within 3%. Similar to the Li/Mo(112) system,[13] and in contrast to the classical Langmuir-Gurney model[28] of alkali atom adsorption, which predicts an elongation of the bond for a higher coverage, the bond length remains nearly constant or is slightly decreased as the coverage is increased. The change in the surface electron density distribution which is manifested in a rapid decrease of the work function for $\Theta \leqslant 0.25$, shows almost no effect on the chemisorption bond length. The calculated lengths are close to the sum of metallic radii[22] for Sr-Mo(3.55 Å), and this suggest a substantial metallic contribution to the bond, larger than that resulting both from measurements[4,5] and calculations[13] for Li-Mo system. This implies, in accordance with experiment, that for Sr adsorption the volume sites (i.e., the positions that would be occupied by the next substrate layer), are most favored. On the

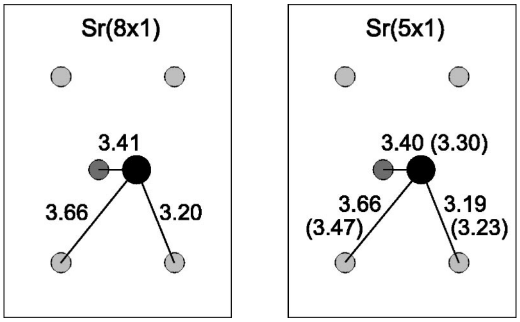

FIG. 5. The Sr-Mo bond lengths (in Å) for the two Sr chain structures on Mo(112). The larger, black circle represents the position of a Sr atom and the darker circle in the middle a Mo atom of the second atomic layer. The measured values (Ref. 5) are given in braces.

relaxed surface the Sr atoms are shifted from these ideal positions, but the calculated shifts are smaller than those determined in experiment.[4]

Energy barriers for diffusion. At elevated temperature of the sample, the Sr atoms can start to diffuse. High energy barriers perpendicular to the furrows will dictate a unidirectional diffusion along the furrows,[32] similarly as for Li/Mo(112).[13] Figure 6 displays the energy barrier, calculated in a 4×2 unit cell, for a Sr atom moving between two volume sites along the furrow. The barrier was determined from the total energy difference of an adatom placed in a succession of locations along the trough ($[11\bar{1}]$ direction) and its energy in a volume site. The calculated barrier is below 80 meV and its magnitude is reduced by 20% compared to Li/Mo(112) system.[13] This shows that a larger size of Sr atom makes the barrier easier to overcome. For Li diffusion on Mo(112) the presence of another Li atom in a neighboring cell decreased the barrier for Li diffusion[13] by $\sim$10%. Thus, the proximity effect of other Sr atoms for an increased coverage may reduce this barrier further. The energetic cost for Sr adatom to diffuse across the atomic rows is an order of magnitude higher than for a diffusion along the rows. Thus, at sufficiently low temperatures, the diffusivity along the furrows is higher by a factor $>10^3$ than across them.[32,33] For typical temperatures ($T\approx750$ K) applied in diffusion experiments[32,33] the barrier for Sr diffusion along the troughs ceases to exist. The calculated barrier heights also consistently explain the fact that the annealing temperatures of 500–700 K, applied in experiment to activate the adatoms, allow one to order the adlayer to form chain structures that are subsequently studied at lower temperatures (100 K).

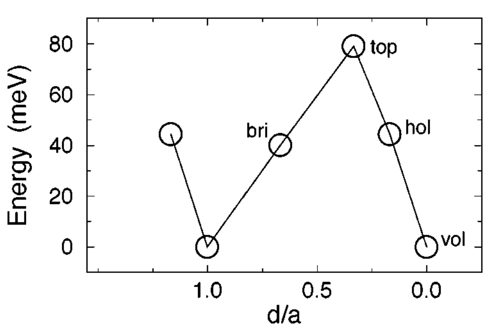

FIG. 6. Energy barrier for Sr atom diffusion between two volume (vol) sites along the furrow. The other labels denote hollow (hol), atop of Mo atom (top), and bridge (bri) sites. The distance is measured in units of surface lattice parameter $a=2.73$ Å.

D. Higher coverage structures ($0.5<\Theta\leq1$)

According to experiment, commensurate $c(2\times2)$ islands corresponding to coverage $\Theta=0.5$ ML, start to grow at much lower global coverage $\Theta=0.23$, coexisting initially with the $p(5\times1)$ domains.[7] In the coverage range $\Theta=0.48-0.53$ a single $c(2\times2)$ phase is observed. This, however, can be easily transformed with small amounts of oxygen impurities into a stable domain of $p(2\times1)$ structures.[34] The role played by the irregularly distributed O doping is difficult to quantify in this type of calculations and is deferred to a future study. Our calculations show (Table II) that the $c(2\times2)$ structure is by 20 meV more stable than the $p(2\times1)$.

For $\Theta>0.53$ ML, the commensurate-incommensurate transition occurs.[7] The appearance of the incommensurate structures is also clear from the inspection of binding energies displayed in Table I. A Sr atom in a $p(2\times1)$ chain is only by 15–20 meV more strongly bound than in the incommensurate structure corresponding to $\Theta=3/5$. Similarly as for Li/Mo(112) system, the Sr atoms which are evenly distributed along the furrow do not remain pinned in their initial positions but are shifted to form three-atom chains along the furrows. This indicates a weakening of the coupling in the original chain directions and a dominating role of interactions along the furrows. It should be noted that the calculation corresponds to zero temperature while the above mentioned phases are observed at finite temperatures. Thus, since the bonds across the furrows are weakened and at room temperature the barrier for activation Sr atoms is reduced, in analogy to the Li/Mo(112) system,[6] the complete rows of Sr atoms in the individual furrows can easily form floating rows, or domains of rows, of evenly spaced atoms. Depending on the oxygen doping, the floating domain can be split along one of the rows and the fragments shifted against each other to form the domain walls of different pattern.

The larger atomic radius of Sr atoms compared to the Mo radius ($\sim$40% larger), in principle, does not allow the formation of the (1×1) adsorbate lattice commensurate with the Mo substrate. However, by placing four Sr atoms in a 4×1 surface unit cell, we found that they remain pinned in their positions along the furrows thus forming a 1 ML commensurate $p(1\times1)$ adlayer structure. This suggests that the Sr atomic radius is substantially reduced compared to the atomic radius in a bulk Sr crystal. Our calculation shows that the binding of atoms in this adlayer is drastically decreased (Table I). It is approximately halved compared to the lower coverage structures discussed earlier. On the other hand, this dramatic change in the binding is not reflected in the adsorbate-substrate distance. The distance of adsorbate layer to the first and second Mo layers is reduced by ~0.12 Å only (~6%).

IV. SUMMARY

The clean Mo(112) surface properties are well reproduced. The structure and energetics of various configurations of electropositive Sr atoms adsorbed on the relaxed Mo(112) surface for different coverages in the range $1/9 \leqslant \Theta \leqslant 1$ are presented and discussed. We found that adsorption of alkaline earths atoms has a stabilizing effect on Mo(112), which is manifested in a reduced topmost layer relaxation. The binding energy of Sr atoms forming chain-structures decreases with increasing coverage. Sr atoms are by about 0.2 eV more strongly bound to the Mo substrate than to Li atoms. Our calculations show, in good agreement with experiment, that $p(8\times1)$ and $p(5\times1)$, which differ in energy by 20 meV, belong to the most stable Sr structures in the range of coverages considered. The possibility of stable Sr(9×1) structures at very low coverages is suggested. The calculated work function variation with Sr adatom coverage, $0 \leqslant \Theta \leqslant 1$, is in very good agreement with experiment and is consistent with the classical Langmuir-Gurney picture of alkali metal adsorption. The energy barriers for Sr atoms diffusion along the furrows are by 20% reduced compared to the barriers encountered by Li adatoms.

ACKNOWLEDGMENTS

This research has been supported by the Academy of Finland through the Centers of Excellence Program (2000-2005) and partially (A.K.) by the Polish Committee for Scientific Research (KBN) Grant No. 1 P03B 047 26. We are grateful to the Centre for Scientific Computing (CSC), Espoo, Finland, for generous allocation of computer resources. A.K. acknowledges with thanks the hospitality of the Laboratory of Physics of HUT during his on leave stay in Helsinki. We thank Herbert Pfnür for useful comments on this work.

[1] J. Kołaczkiewicz and E. Bauer, Surf. Sci. **144**, 477 (1984).
[2] S. Stepanowskyi, I. Ubogyi, and J. Kołaczkiewicz, Surf. Sci. **411**, 176 (1998).
[3] O. M. Braun and V. K. Medvedev, Usp. Fiz. Nauk **157**, 631 (1989) [Sov. Phys. Usp. **32**, 328 (1989)] .
[4] D. Kolthoff and H. Pfnür, Surf. Sci. **457**, 134 (2000).
[5] D. Kolthoff and H. Pfnür, Surf. Sci. **459**, 265 (2000).
[6] A. Fedorus, D. Kolthoff, V. Koval, I. Lyuksyutov, A. G. Naumovets, and H. Pfnür, Phys. Rev. B **62**, 2852 (2000).
[7] A. Fedorus, G. Godzik, V. Koval, A. Naumovets, and H. Pfnür, Surf. Sci. **460**, 229 (2000).
[8] G. Godzik, T. Block, and H. Pfnür, Phys. Rev. B **67**, 125424 (2003).
[9] V. K. Medvedev and I. N. Yakovkin, Fiz. Tverd. Tela (S.-Peterburg) **21**, 313 (1979) [Sov. Phys. Solid State **21**, 187 (1979)].
[10] J. Neugebauer and M. Scheffler, Phys. Rev. B **46**, 16067 (1992).
[11] B. Gumhalter and W. Brenig, Surf. Sci. **336**, 326 (1995).
[12] F. Bagehorn, J. Lorenc, and C. Oleksy, Surf. Sci. **349**, 165 (1996).
[13] A. Kiejna and R. M. Nieminen, Phys. Rev. B **66**, 085407 (2002).
[14] R. Drautz, R. Singer, and M. Fähnle, Phys. Rev. B **67**, 035418 (2003).
[15] P. Hohenberg and W. Kohn, Phys. Rev. **136**, B864 (1964).
[16] W. Kohn and L. J. Sham, Phys. Rev. **140**, 1133A (1965).
[17] J. P. Perdew, J. A. Chevary, S. H. Vosko, K. A. Jackson, M. R. Pederson, D. J. Singh, and C. Fiolhais, Phys. Rev. B **46**, 6671 (1992); **48**, 4978 (1993).
[18] G. Kresse and D. Joubert, Phys. Rev. B **59**, 1758 (1999).
[19] VASP was developed at the Institut für Theoretische Physik of the Technische Universität Wien: G. Kresse and J. Hafner, Phys. Rev. B **47**, R558 (1993); **49**, 14 251 (1994); G. Kresse and J. Furthmüller, Phys. Rev. B **54**, 11 169 (1996); Comput. Mater. Sci. **6**, 15 (1996).
[20] H. J. Monkhorst and J. D. Pack, Phys. Rev. B **13**, 5188 (1976).
[21] M. Methfessel and A. T. Paxton, Phys. Rev. B **40**, 3616 (1989).
[22] Ch. Kittel, *Introduction to Solid State Physics*, 7th ed. (Wiley, New York, 1996).
[23] J. G. Che, C. T. Chan, W.-E. Jian, and T. C. Leung, Phys. Rev. B **57**, 1875 (1998).
[24] R. Smoluchowski, Phys. Rev. **60**, 661 (1941).
[25] M. W. Finnis and V. Heine, J. Phys. F: Met. Phys. **4**, L3 (1974).
[26] D. Kolthoff, H. Pfnür, A. G. Fedorus, V. Koval, and A. G. Naumovets, Surf. Sci. **439**, 224 (1999).
[27] S. Berge, P. O. Gartland, and B. J. Slagsvold, Surf. Sci. **43**, 275 (1974).
[28] R. D. Diehl and R. McGrath, J. Phys.: Condens. Matter **9**, 951 (1997).
[29] A. Kiejna and K. F. Wojciechowski, *Metal Surface Electron Physics* (Pergamon, Oxford, 1996).
[30] K. Swamy, C. Deisl, A. Menzel, R. Beer, S. Penner, and E. Bertel, Phys. Rev. B **65**, 121404(R) (2002).
[31] H. Pfnür (private communication).
[32] A. G. Naumovets, M. V. Paliy, Yu. S. Vedula, A. T. Loburets, and N. B. Senenko, Prog. Surf. Sci. **48**, 59 (1995).
[33] A. T. Loburets, A. G. Naumovets, and Yu. S. Vedula, in *Surface Diffusion: Atomistic and Collective Processes* (Plenum, New York, 1997), p. 509.
[34] G. Godzik, H. Pfnür, and I. Lyuksyutov, Europhys. Lett. **56**, 67 (2001).